Substantial Increases in Eastern Amazon and Cerrado Biomass Burning-Sourced Tropospheric Ozone

Richard J. Pope[1,2] iD, **Stephen R. Arnold[1]** iD, **Martyn P. Chipperfield[1,2]** iD, **Carly L. S. Reddington[1]** iD, **Edward W. Butt[1]**, **Tim D. Keslake[1,2]**, **Wuhu Feng[1,3]** iD, **Barry G. Latter[4]**, **Brian J. Kerridge[4]**, **Richard Siddans[4]**, **Luciana Rizzo[5]**, **Paulo Artaxo[6]** iD, **Mehliyar Sadiq[7]** iD, and **Amos P. K. Tai[7,8]** iD

[1]School of Earth and Environment, University of Leeds, Leeds, UK, [2]National Centre for Earth Observation, University of Leeds, Leeds, UK, [3]National Centre for Atmospheric Sciences, University of Leeds, Leeds, UK, [4]Remote Sensing Group, STFC Rutherford Appleton Laboratory, Chilton, United Kingdom, [5]Department of Environmental Sciences, Universidade Federal de Sao Paulo, Diadema, Brazil, [6]Department of Applied Physics, Institute of Physics, University of Sao Paulo, Brazil, [7]Earth System Science Programme, Faculty of Science, and Institute of Environment, Energy and Sustainability, The Chinese University of Hong Kong, Hong Kong, [8]State Key Laboratory of Agrobiotechnology, The Chinese University of Hong Kong, Hong Kong

Abstract The decline in Amazonian deforestation rates and biomass burning activity (2001–2012) has been shown to reduce air pollutant emissions (e.g., aerosols) and improve regional air quality. However, in the Cerrado region (savannah grasslands in northeastern Brazil), satellite observations reveal increases in fire activity and tropospheric column nitrogen dioxide (an ozone precursor) during the burning season (August-October, 2005–2016), which have partially offset these air quality benefits. Simulations from a 3-D global chemistry transport model (CTM) capture this increase in NO_2 with a surface increase of ~1 ppbv per decade. As there are limited long-term observational tropospheric ozone records, we utilize the well-evaluated CTM to investigate changes in ozone. Here, the CTM suggests that Cerrado region surface ozone is increasing by ~10 ppbv per decade. If left unmitigated, these positive fire-sourced ozone trends will substantially increase the regional health risks and impacts from expected future enhancements in South American biomass burning activity under climate change.

1. Introduction

Fire is a widely used method for land clearance in the tropics, allowing rapid conversion of regions of natural vegetation to agricultural land (Cochrane, 2003). In the Amazon, these deforestation practices led to a 15–20% decrease in forest cover between 1976 and 2010 (Aragão et al., 2014; Davidson et al., 2012; Hansen et al., 2013). Vegetation fires are a large source of reactive trace gases and aerosol to the Amazon atmosphere (Bela et al., 2015; Hodgson et al., 2018; Sena & Artaxo, 2015; Ward et al., 1992), especially during the dry season, with substantial impacts on the atmospheric radiation balance (Kolusu et al., 2015; Scott et al., 2018; Sena & Artaxo, 2015; Thornhill et al., 2018) and surface air quality (Artaxo et al., 2013; Johnston et al., 2012; Jacobson et al., 2014; Reddington et al., 2015; Pacifico et al., 2015).

Over the period 2001 to 2012, deforestation rates in Brazil decreased by ~40% (Hansen et al., 2013) leading to improvements in particulate air quality (Reddington et al., 2015). These decreasing deforestation rates correlated with reductions in satellite-observed aerosol optical depth (AOD) over the Amazon, which were attributed to significant reductions in surface emissions of aerosol from deforestation fires (Reddington et al., 2015). Reductions in surface $PM_{2.5}$ (mass of particulate matter with diameter less than 2.5 μm) concentrations, resulting from the reduction in fire emissions, were estimated to prevent 400–1,700 premature deaths annually in South America. The reduction in fire activity is particularly evident in the arc of deforestation, around the southern edge of the Amazon Basin, where the majority of Amazon deforestation fires occur (van der Werf et al., 2017). Satellite-observed fire-burned area (FBA) in this region has decreased by 0.25–0.5%/year between 1998 and 2015 (Andela et al., 2017). Despite these reductions in the arc of deforestation, FBA in northeastern Brazil has increased by 0.5–1.0%/year, resulting in increased regional pollutant emissions (Andela et al., 2017; Chen et al., 2013). This region represents the transition biome between the eastern Amazon, the Cerrado grasslands, and the Caatinga desert vegetation (Santo et al., 2017). However, this region is predominantly covered by savannah grasslands, and hereafter, we refer to it as the

"Cerrado Region" (i.e., the Cerrado biome in Figures 1a and 1b and the boarding regions of the Caatinga and Amazonia biomes).

As a major source of ozone precursors (nitrogen oxides [NO_x] and volatile organic compounds (VOCs), vegetation fires have been observed to lead to enhancement in tropospheric ozone concentrations (Artaxo et al., 2013; Bela et al., 2015; Jaffe & Wigder, 2012; Kirchhoff & Marinho, 1994; Kirchhoff et al., 1996). Tropospheric ozone is an important air pollutant, which causes adverse effects on human health (Doherty et al., 2017; Jerrett et al., 2009), crops (Hollaway et al., 2012; Van Dingenen et al., 2009), and natural vegetation (Sitch et al., 2007). Deforestation fires tend to be large in scale (due to extensive aboveground biomass) with a greater amount of smoldering, while savannah fires tend to be smaller and burn at higher temperatures with more flaming combustion (Alencar et al., 2015; Hodgson et al., 2018; Longo et al., 2009). Consequently, these different fire characteristics can result in very different emissions. For instance, emission factors (i.e., mass of trace gas/aerosol emitted per mass of dry matter burnt) for deforestation fires release larger quantities of primary aerosol emissions (13.0 g/kg) than savannah fires (8.5 g/kg), while the converse is the case for NO_x emissions (deforestation emission factor = 2.55 g/kg and savannah emission factor = 3.9 g/kg) (Akagi et al., 2011). Therefore, understanding how changes in fire activity impact NO_x and ozone pollution requires knowledge of the underlying vegetation type and emission characteristics.

It is only recently, in the satellite era, that space-borne observations from various missions have made it possible to study long-term changes in global tropospheric composition. Here, we present the first study using these long-term (2005–2016) records, in conjunction with a chemistry transport model (CTM), to investigate the impact of changing wildfire/biomass burning (BB) activity on tropospheric ozone air quality across the Amazon during the BB season (August-September-October [ASO]). We exploit satellite measurements of tropospheric nitrogen dioxide (NO_2) and fire activity, as well as new state-of-the-art lower tropospheric ozone retrievals. Our focus is on detecting and analyzing trends in tropospheric/surface ozone and its precursors to investigate the impact on regional air quality. Section 2 introduces the satellite measurements and CTM used in this study, section 3 presents our results, and the conclusions are discussed in section 4.

2. Methods and Data

2.1. Satellite Data

We use satellite measurements of tropospheric column NO_2 ($TCNO_2$) and subcolumn (0–6 km) ozone (SCO_3) from the Ozone Monitoring Instrument (OMI) from 2005–2016. OMI is a nadir viewing instrument onboard NASA's Aura satellite (2004 to present) (Boersma et al., 2007). The OMI $TCNO_2$ data were downloaded as Level 2 swath data from the Tropospheric Emissions Monitoring Internet Service (www.temis.nl). The SCO_3 data were provided by the Rutherford Appleton Laboratory, which uses an optimal estimation technique (Miles et al., 2015) to produce a state-of-the-art product with peak vertical sensitivity in the lower troposphere. Aura is polar orbiting with an approximate local overpass time of 13.30, and OMI has nadir-viewing spectral ranges of 270–500 nm (Boersma et al., 2011). All data sets have been quality controlled for geometric cloud fraction less than 0.2, good quality flags, and the OMI row anomalies (Braak, 2010) where applicable. Detailed analysis of $TCNO_2$ retrieval uncertainties is provided by Boersma et al. (2004), while Bousserez (2014) quantifies the impact of BB aerosol uncertainty on retrieved $TCNO_2$. Miles et al. (2015) provide error/uncertainty analysis on the retrieval scheme used for the Rutherford Appleton Laboratory OMI SCO_3 product. These satellite data sets were mapped onto high-resolution spatial grids of $0.05° \times 0.05°$ for $TCNO_2$ and $1.0° \times 1.0°$ for SCO_3 (Pope et al., 2018). Global Ozone Monitoring Experiment-2 $TCNO_2$ data were also acquired from TEMIS as a Level 3 monthly mean gridded product for ASO 2007–2016, to confirm that the Cerrado Region $TCNO_2$ positive trends (Figure 2a) were realistic and not an artifact of the OMI row anomaly.

We use two different satellite-derived fire activity data sets to investigate regional patterns in fires and their trends over time. These are FBA from the Global Fire Emissions Database (GFED vn4.0; van der Werf et al., 2017) and fire radiative power (FRP) from the Global Fire Assimilation System (vn1.2; Kaiser et al., 2012). Both fire products are derived from Moderate Resolution Imaging Spectroradiometer measurements, onboard NASA's Aqua and Terra satellites (Remer et al., 2005), and are used to produce gas-phase and aerosol emissions from fires through application of emissions factors (Wooster et al., 2018). While Global Fire
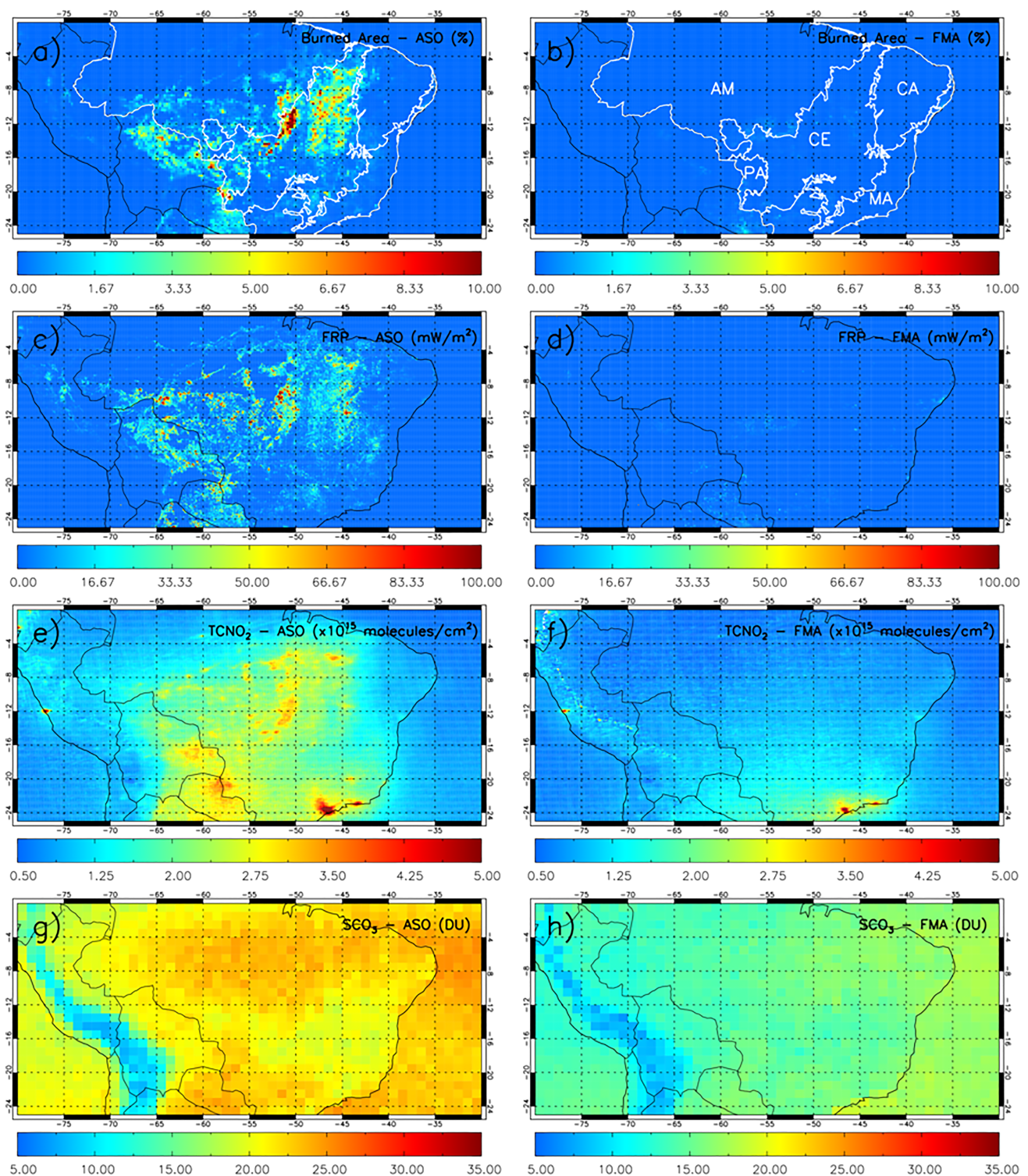
Figure 1. Mean satellite fire activity and tropospheric composition (2005–2016) for August-September-October (ASO; panels a, c, e, and g) and February-March-April (FMA; panels b, d, f, and h). (a) and (b) show GFED Fire-Burned Area (FBA, %), (c) and (d) show GFAS Fire Radiative Power (FRP, mW/m^2), (e) and (f) show OMI tropospheric column NO$_2$ (TCNO$_2$, 10^{15} molecules per cm^2), and (g) and (h) show OMI subcolumn (0–6 km) ozone (SCO$_3$, Dobson units [DU]). The white-outlined regions in (a) and (b) are the Brazilian biomes (Global Forest Watch, 2019) with their corresponding labels in white. AM = Amazonia; CA = Caatinga; CE = Cerrado; MA = Mata Atlantica; PA = Pantanal.

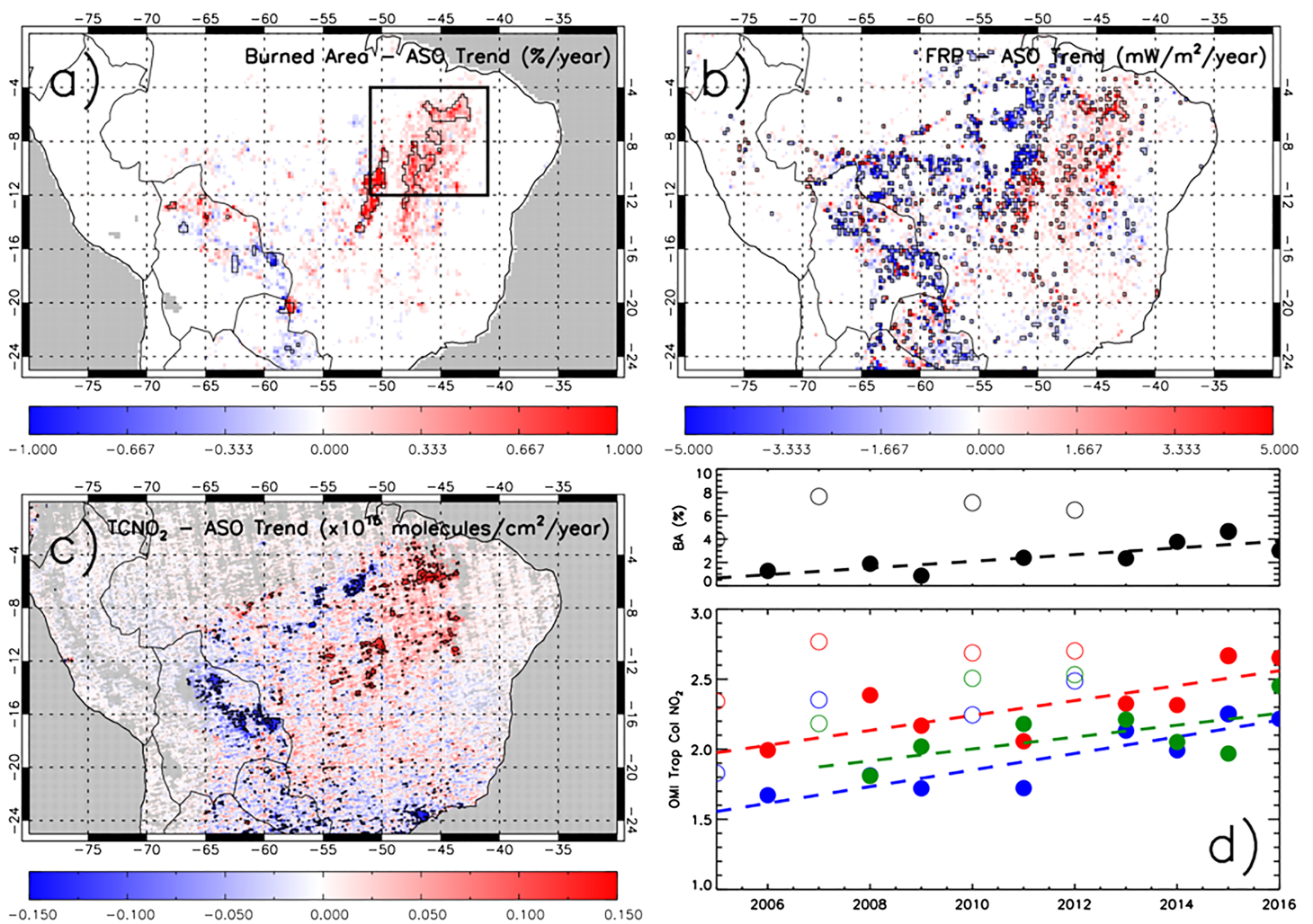**Figure 2.** Linear trends in the burning-season (ASO) average for each year, between 2005 and 2016, for (a) GFED FBA (%/year), (b) GFAS FRP (mW/m^2/year), and (c) OMI TCNO$_2$ (10^{15} molecules/cm^2/year). Black polygon-outlined regions highlight significant trends at and above the 90% confidence level (>90% CL). (d) shows significant (99% CL) regional trends (black box in (a)) in FBA (%/year), OMI TCNO$_2$ (10^{15} molecules/cm^2/year), GOME-2 TCNO$_2$ (10^{15} molecules/cm^2/year), and OMI TCNO$_2$ sampled under FBA pixels of >1% (10^{15} molecules/cm^2/year) represented by the black, blue, green, and red dashed lines, respectively. Open circles represent extreme drought/anomalous fire years and are not included in trend analysis.

Assimilation System only provides FRP and total emissions, GFED provides information on different vegetation types burned, including contributions from deforestation and savannah fires.

2.2. TOMCAT Model Setup and Evaluation

The TOMCAT global off-line CTM (Chipperfield, 2006) is forced by ECMWF ERA-Interim reanalysis meteorology (Dee et al., 2011) and has a horizontal spatial resolution of 2.8° × 2.8° with 31 vertical levels up to 10 hPa. The model includes detailed tropospheric chemistry, including 229 gas-phase reactions and 82 advected tracers (Monks et al., 2017), and heterogeneous chemistry driven by size-resolved aerosol from the GLOMAP module (Mann et al., 2010). Simulations used here include anthropogenic emissions from the Coupled Model Intercomparison Project Phase 6 (Hosely et al., 2018) and fire emissions from GFED vn4.0 (van der Werf et al., 2017). Biogenic VOCs emissions are from the Chemistry-Climate Model Initiative (Morgenstern et al., 2017).

TOMCAT surface/tropospheric ozone was evaluated against surface observations from Manaus (60.2°W, 2.6°S) in the Amazon (2010–2011). During the BB season (ASO), the model successfully captures peak observed surface ozone concentrations of 13–15 ppbv. However, between January and May, there is

systematic positive bias of ~5 ppbv (although this is within the observational variability). Comparisons with aircraft observations from the South AMerican Biomass Burning Analysis campaign (Darbyshire et al., 2019) (September-October 2012) show the model successfully reproduces the boundary layer vertical ozone profile between 30 and 45 ppbv, with a slight positive bias of 2–3 ppbv. These observations and comparison are also consistent with ozonesondes from Natal (2007–2008). More details on the model evaluation are located in supporting information section S2.

Overall, the TOMCAT model successfully captures the Amazon ozone seasonality and absolute concentrations in the lower troposphere, giving confidence in the ozone simulations used to investigate long-term changes in surface ozone in the following analysis.

3. Results

3.1. Satellite Fire Emission Signals and Trend Detection

The period of peak fire activity over the Amazon occurs during ASO (Hodgson et al., 2018; Kaiser et al., 2012; van der Werf et al., 2017), when FBA (Figure 1a) and FRP (Figure 1c) reach over 10% and 100 mW/m^2, respectively. In contrast, during the non-BB season (February-March-April [FMA]), there are minimal fire signals, peaking at <1% (Figure 1b) and 10 mW/m^2 (Figure 1d). Substantial fire-related TCNO$_2$ signals (2.5–4.0 $\times$ 10^{15} molecules per cm^2; Figure 1e) are present across the Amazon during ASO, while in FMA, TCNO$_2$ concentrations are less than 1.0 $\times$ 10^{15} molecules per cm^2 (Figure 1f). During ASO peak, TCNO$_2$ is located over the Cerrado region where savannah-type fires (both natural and anthropogenic) burn at high temperatures (Hodgson et al., 2018) releasing large quantities of NO$_x$ (Akagi et al., 2011). There will also be contributions from deforestation and agricultural fires (e.g., de Araújo et al., 2019). In comparison, TCNO$_2$ hot spots over large cities (e.g., São Paulo and Rio De Janeiro) show limited seasonality, remaining above 5.0 $\times$ 10^{15} molecules per cm^2 year-round. The SCO$_3$ ASO signal is more homogeneous, consistent with ozone being a secondary NO$_x$-induced pollutant formed downwind of source regions. A clear SCO$_3$ enhancement (22–25 Dobson units [DU]) is present during ASO over the Amazon compared with FMA (12–18 DU). SCO$_3$ over the South Atlantic is also elevated (over 22 DU) in ASO as a result of ozone-enriched outflow from the southern African BB (Moxim & Levy, 2000).

A long-term trend analysis (Figure 2) shows significant increases in both fire activity and TCNO$_2$ across the Cerrado Region. Trends are calculated using a linear least squares fit over the ASO composition average for each year between 2005 and 2016, where we remove extreme drought/anomalous fire years (e.g., 2005, 2007, 2010, and 2012; hereafter defined as ED-AF). Though the 2015 intense positive El Niño-Southern Oscillation event substantially enhanced drought conditions in the Central Amazon (Anderson et al., 2018), it had a limited impact on fire activity over our primary region of interest (black box in Figure 2a; see section S1). Hence, 2015 was not defined as ED-AF (see section S1). We follow the approach of Reddington et al. (2015) and remove ED-AF years from our analysis as they represent different emission regimes when compared to the normal state (Aragão et al., 2014). For aerosol emissions, Reddington et al. (2015) found that ED-AF years were 1.5–2.8 times greater than normal years, while for NO$_x$ emissions, we find a factor increase of 14–15. This avoids skewing of the long-term trends due to larger than usual fire activity and tropospheric pollutant loading in those years. Black polygon-outlined regions in Figure 2 show significant trends at and above the 90% confidence level (>90% CL; *trend*/σ_{trend} > 1.645). Artificial background TCNO$_2$ trends (i.e., OMI row anomaly; Braak, 2010) have been removed from the OMI time series (section S1). Where significant TCNO$_2$ trends exist, there are insignificant trends in the stratospheric slant NO$_2$ column and in the tropospheric air mass factor.

Significant positive trends in FBA (Figure 2a), FRP (Figure 2b), and TCNO$_2$ (Figure 2c) range between 0.3% and 0.7% per year, 2 and 5 mW/m^2/year, and 0.1 and 0.15 $\times$ 10^{15} molecules per cm^2/year, respectively, potentially driven by changes in Cerrado savannah-type fire activity. Given that all three data sets have spatially consistent trends, it provides us with confidence that the detected TCNO$_2$ trends are related to fire activity. In the arc of deforestation region, significant (>90% CL) negative trends are also found in all three data sets, consistent with previous studies (Reddington et al., 2015), which identified decreases in deforestation fires and satellite-observed AOD between 2001 and 2012. Though the negative FBA and TCNO$_2$ signals are spatially less extensive than those of the FRP and AOD negative trends.
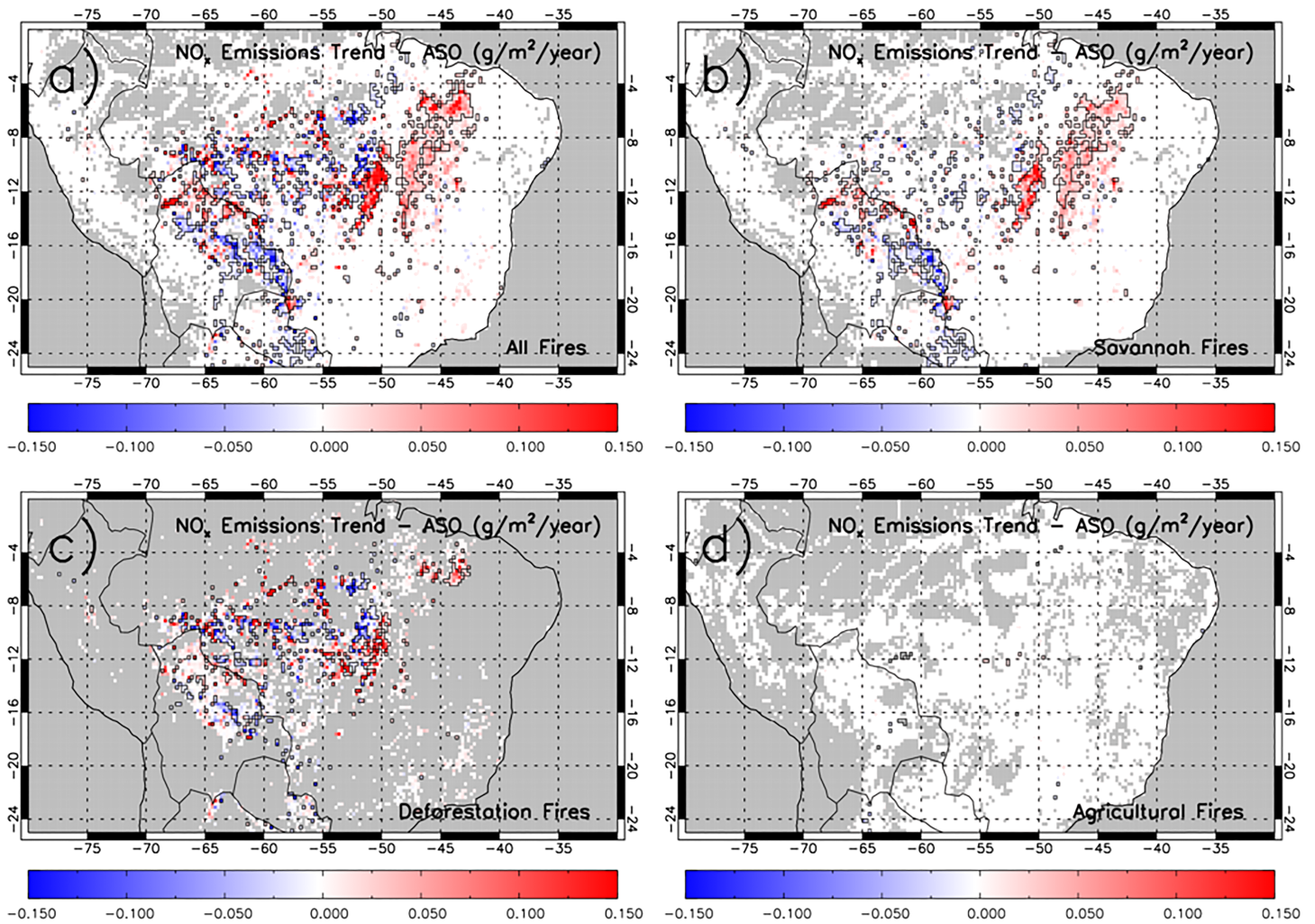
Figure 3. Trends in GFED NO_x (g/m^2/year) ASO total emissions between 2005 and 2016 for (a) all fires, (b) savannah fires, (c) deforestation fires, and (d) agricultural fires. Black polygon-outlined regions indicate significant trends above the 90% CL.

As the significant fire activity and $TCNO_2$ positive trends over the Cerrado Region are spatially sporadic and disjointed, regional trends (Figure 2d) in FBA and $TCNO_2$ were determined from the black-outlined region in Figure 2a. The variability (standard deviation) in the regional FBA and $TCNO_2$ typically ranges between 150% and 190% and 40% and 60% of the mean values, respectively, in non-ED-AF years. Here, there are significant regional trends (99% CL) in both FBA and $TCNO_2$. The $TCNO_2$ regional trend from the Global Ozone Monitoring Experiment-2 satellite instrument also increases significantly over time (2007–2016), supporting the OMI $TCNO_2$ results. By subsampling OMI $TCNO_2$ under pixels with FBA >1.0%, concentrations are larger by approximately 0.5×10^{15} molecules per cm^2, highlighting a similar significant positive trend (red dashed line). This strongly suggests that increasing regional $TCNO_2$ concentrations are being driven by increased fire activity as $TCNO_2$ is larger in fire-classified pixels with a consistent significant positive trend.

Analysis of trends in GFED NO_x emissions, which are based on FBA, for ASO indicates that increases in GFED-defined savannah-type fires are likely responsible for the increases in $TCNO_2$ over the Cerrado Region. Figure 3a shows the GFED NO_x emissions trends for all fire types for 2005–2016 with ED-AF years removed and shows significant positive trends (0.05–0.15 g/m^2/year) over the Cerrado Region, consistent with the FBA, FRP, and $TCNO_2$. When split into fire types, agricultural fires (Figure 3d) show negligible trends, while deforestation fires (Figure 3c) give spatially incoherent trends across the Amazon (partial spatial agreement with savannah fires over portions of the Cerrado Region, e.g., around 50°W, 12°S suggesting a
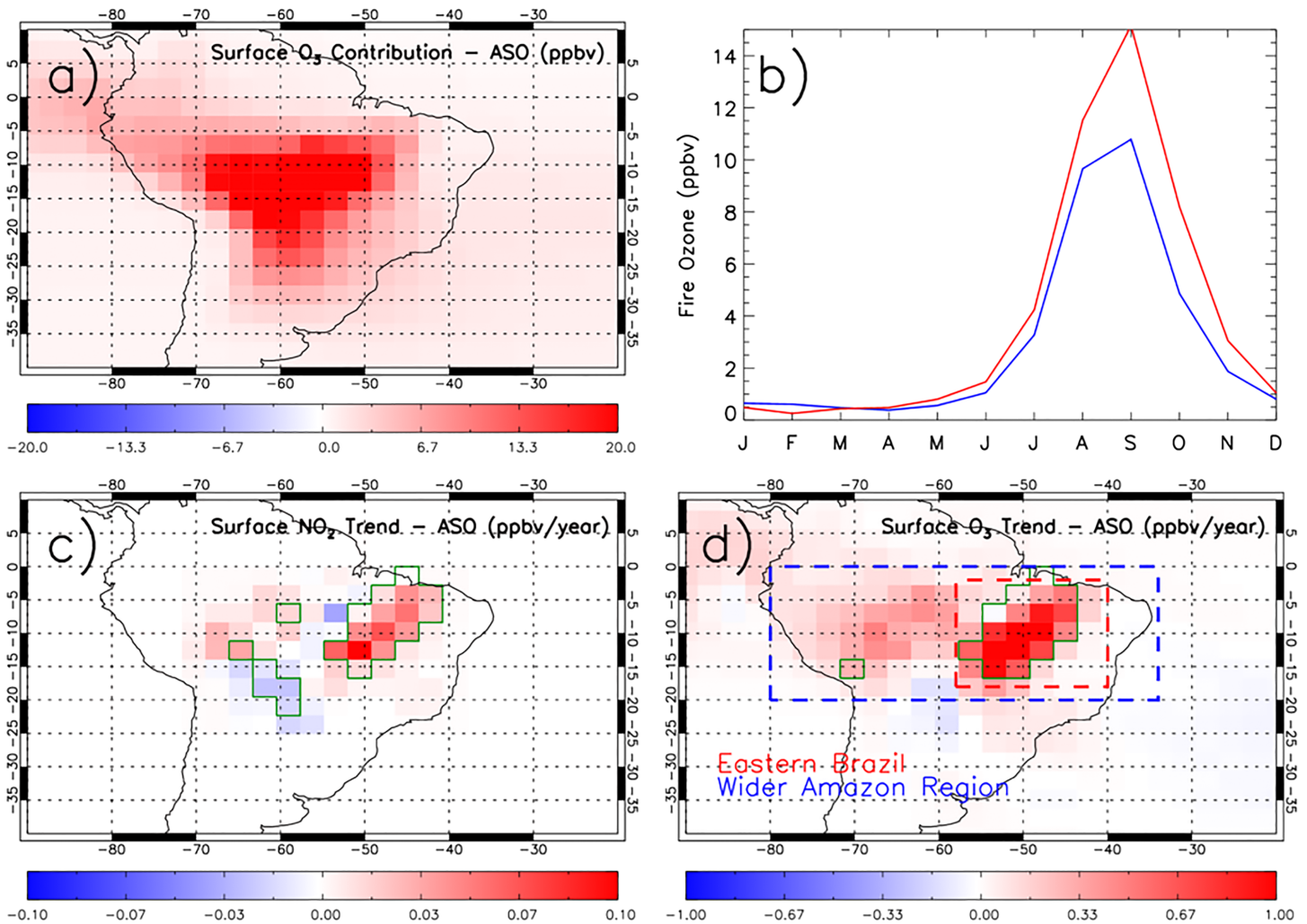
Figure 4. (a) Average (ASO, 2005–2016) contribution of fire-sourced ozone to Amazon surface ozone concentrations (ppbv). (b) Seasonal cycle in surface fire-sourced ozone (ppbv) in the Eastern Brazil and Wider Amazon regions (red and blue dashed regions in (d)). Trends in TOMCAT model surface (c) NO_2 (ppbv/year) and (d) ozone (ppbv/year) for the ASO average between 2005 and 2016. Green polygon-outlined areas show regions of significant trends above the 90% CL.

range of different vegetation fire types driving the positive trends seen in Figures 2 and 3). However, the significant positive NO_x emission trends (0.05–0.1 g/m^2/year) from savannah fires (Figure 3b) are closely related to the magnitude and spatial pattern of the trends in Figure 3a. Though it should be noted that the GFED fire-type classifications can be subject to uncertainties (van der Werf et al., 2017). Missed or false fire detections will also introduce further emission uncertainties (e.g., particulate emissions; Reddington et al., 2016).

3.2. Model simulated NO_2 and Ozone

TOMCAT model simulations (2005–2016; Figure 4), using annual varying GFED vn4.0 fire emissions, are used to investigate the impact of increased fire activity (predominantly savannah-type fires) on air quality over the Cerrado region and the wider surrounding Amazon area, given the limited observational spatial and temporal coverage. Neither the surface nor aircraft data provide long-term records, and the ozonesondes are from Natal (a coastal city). The OMI SCO$_3$ observations provide valuable seasonal information over the wider Amazon but are not sensitive enough to detect finer-scale changes (e.g., for the Cerrado region) in ozone with time. However, evaluation of TOMCAT tropospheric ozone using these observations (surface sites, aircraft data, and ozonesondes; see section S2) show that the model is able to capture the surface ozone seasonal cycle and reproduce the lower tropospheric vertical profile.

Over the 2005–2016 period, fire-sourced ozone contributes approximately an extra 10–15 ppbv to Amazon surface ozone concentrations during the BB season. Figure 4a shows the difference between the TOMCAT "fire-on" and "fire-off" simulations, where fires have substantially contributed to the surface ozone budget in ASO, consistent with the ozone seasonality in the observations. During ASO, the 2005–2016 average surface concentrations range between 40 and 50 ppbv in the "fire-on" simulation while decreasing to under 20 ppbv when fire sources are switched off ("fire-off"; see section S3). The red and blue dashed regions in Figure 4d represent the Eastern Amazon and Wider Amazon, respectively, and highlight regions where we have detected long-term fire-sourced ozone enhancements. During ASO, the domain average fire-source ozone contribution ranges between 10–15 and 5–11 ppbv for the Eastern Amazon and Wider Amazon regions (Figure 4b). This implies that approximately 50–60% of the ASO surface ozone is from fire sources (see section S3). The ASO Eastern Amazon ozone contributions tend to be larger as more NO$_x$ is emitted from the predominantly savannah-type fire regimes (i.e., Figure 3b), when compared with the Wider Amazon region.

Trends in model surface ASO mean NO$_2$ show significant (>90% CL) increases (>0.1 ppbv/year) over the Cerrado region and decreases (−0.03 to −0.01 ppbv/year) in the arc of deforestation (Figure 4c). As expected, the short NO$_2$ lifetime means that these trends are highly correlated with those in GFED v4.0 NO$_x$ fire emissions (Figure 3a). The significant increase in Cerrado fire-related NO$_x$, in the presence of VOC concentrations (both biogenic emissions from vegetation and emissions from fires), yields significant increases in simulated ozone (over 1.0 ppbv/year; Figure 4d). However, insignificant decreases (−0.2 to 0.0 ppbv/year) and increases (0.1–0.3 ppbv/year) occur over the arc of deforestation and western Amazon, respectively. Model-simulated eastern Brazil surface NO$_2$ and ozone (same region in Figure 2a and section S3) also show significant regional positive trends (>90% CL).

4. Discussion and Conclusions

Overall, our results show that there has been a significant increase in fire activity in the Cerrado region (savannah grasslands) of northeastern Brazil, between 2005 and 2016, yielding substantial increases in fire-related tropospheric pollutants (i.e., NO$_2$ and ozone). This is important as it highlights different behavior compared with the "arc of deforestation" region (the southwestern Amazon reaching to the northeastern flank), where a decline in deforestation fires has yielded lower particulate matter emissions and reduced the corresponding health risks (Reddington et al., 2015). As there are limited observations of surface/tropospheric ozone in the Amazon, well-evaluated model simulations offer a method to quantify long-term changes in surface ozone concentrations. In the Cerrado region, TOMCAT simulations suggest considerable long-term increases in fire-sourced surface ozone (~1.0 ppbv/year equating to ~10–12 ppbv regionally over the study period), predominantly from increased burning of savannah grasslands in the Cerrado Region, but also with contributions from deforestation fires.

Should these fire activities continue to intensify, as is currently seen in Brazil (Terrabrasilia, 2019; NASA, 2019), the health risks and socioeconomic impacts associated with fire-sourced ozone pollution may increase substantially. This will be confounded by the high probability of more frequent and intense drought BB from future climate change (Page et al., 2017) and land use change (Fonseca et al., 2019), as well as expected increases in the South American population (United Nations, 2017). The enhanced ozone will also likely further damage vegetation and reduce photosynthesis (Pacifico et al., 2015; Sitch et al., 2007) leading to reductions in crop yields (Hollaway et al., 2012). These effects combined could have substantial impacts on natural vegetation, agriculture, and public health, with potential degradation in ecosystem services and economic losses. Therefore, targeted policies on controlling Cerrado BB would be benefical to generate local and regional air quality improvements with associated public and ecological health benefits.

References

Akagi, S. K., Yokelson, R. J., Wiedinmyer, C., Alvarado, M. J., Reid, J. S., Karl, T., et al. (2011). Emission factors for open and domestic biomass burning for use in atmospheric models. *Atmospheric Chemistry and Physics*, *11*(9), 4039–4072. https://doi.org/10.5194/acp-11-4039-2011

Alencar, A. A., Brando, P. M., Asner, G. P., & Putz, F. E. (2015). Landscape fragmentation, server drought, and the new Amazon forest fire regime. *Ecological Applications*, *25*(6), 1493–1505. https://doi.org/10.1890/14-1528.1

Andela, N., Morton, D. C., Giglio, L., Chen, Y., van der Werf, G. R., Kasibhatla, P. S., et al. (2017). A human-driven decline in global burned area. *Science*, *356*(6345), 1356–1362. https://doi.org/10.1126/science.aal4108

Aragão, L. E. O. C., Poulter, B., Barlow, J. B., Anderson, L. O., Malhi, Y., Saatchi, S., et al. (2014). Environmental change and the carbon balance of Amazonian forests. *Biological Reviews*, *89*(4), 913–931. https://doi.org/10.1111/brv.12088

Artaxo, P., Rizzo, L. V., Brito, J. F., Barbosa, H. M. J., Arana, A., Sena, E. T., et al. (2013). Atmospheric aerosols in Amazonia and land use change: From natural biogenic to biomass burning conditions. *Faraday Discussions*, *165*, 203–235. https://doi.org/10.1039/C3FD00052D

Bela, M. M., Longo, K. M., Freitas, S. R., Moreira, D. S., Beck, V., Wofsy, S. C., et al. (2015). Ozone production and transport over the Amazon basin during the dry-wet and wet-dry transition seasons. *Atmospheric Chemistry and Physics*, *15*(2), 757–782. https://doi.org/10.5194/acp-15-757-2015

Boersma, K. F., Eskes, H. J., & Brinksma, E. J. (2004). Error analysis for tropospheric NO_2 retrievals from space. *Journal of Geophysical Research*, *109*, D04311. https://doi.org/10.1029/2003JD00362

Boersma, K. F., Eskes, H. J., Veefkind, J. P., Brinksma, E. J., van der A, R. J., Sneep, M., et al. (2007). Near-real time retrievals of tropospheric NO_2 from OMI. *Atmospheric Chemistry and Physics*, *7*(8), 2103–2118. https://doi.org/10.5194/acp-7-2103-2007

Boersma, K. F., Eskes, H. J., Veefkind, J. P., Brinksma, E. J., van der A, R. J., Sneep, M., et al. (2011). An improved tropospheric NO_2 column retrieval algorithm for the Ozone Monitoring Instrument. *Atmospheric Measurement Techniques*, *7*(8), 2103–2118. https://doi.org/10.5194/acp-7-2103-2007

Bousserez, N. (2014). Space-based retrieval of NO_2 over biomass burning regions: Quantifying and reducing uncertainties. *Atmospheric Measurement Techniques*, *7*, 3431–3444. https://doi.org/10.5194/amt-7-3431-2014

Braak, R. (2010). Row anomaly flagging rules lookup table, KNMI Technical Document TN-OMIE-KNMI-950.

Chen, Y., Morton, D. C., Jin, Y., Collatz, G. J., Kasibhatla, P. S., van der Werf, G. R., et al. (2013). Long-term trends and interannual variability of forest, savannah and agricultural fires in South America. *Carbon Management*, *4*(6), 617–638. https://doi.org/10.4155/cmt.13.61

Chipperfield, M. P. (2006). New version of the TOMCAT/SLIMCAT off-line chemistry transport model: Intercomparison of stratospheric trace experiments. *Quarterly Journal of the Royal Meteorological Society*, *132*, 1179–1203. https://doi.org/10.1256/qj.05.51

Cochrane, M. A. (2003). Fire sciences for rainforests. *Nature*, *421*(6926), 913–919. https://doi.org/10.1038/nature01437

Darbyshire, E., Morgan, W. T., Allan, J. D., Liu, D., Flynn, M. J., Dorsey, J. R., et al. (2019). The vertical distribution of biomass burning pollution over tropical South America from aircraft in situ measurements during SAMBBA. *Atmospheric Chemistry and Physics*, *19*(9), 5771–5790. https://doi.org/10.5194/acp-19-5771-2019

Davidson, E. A., de Araujo, A. C., Artaxo, P., Balch, J. K., Brown, I. F., Bustamante, M. M. C., et al. (2012). The Amazon Basin in transition. *Nature*, *481*(7381), 321–328. https://doi.org/10.1038/nature10717

de Araújo, M. L. S., Sano, E. E., Bolfe, E. L., Santos, J. R. N., dos Santos, J. S., & Silva, F. B. (2019). Spatiotemporal dynamics of soybean crop in the Matopiba region, Brazil (1990–2015). *Land Use Policy*, *80*, 57–67. https://doi.org/10.1016/j.landusepol.2018.09.040

Dee, D. P., Uppala, S. M., Simmons, A. J., Berrisford, P., Poli, P., Kobayashi, S., et al. (2011). The ERA-Interim reanalysis: Configuration and performance of the data assimilation system. *Quarterly Journal of the Royal Meteorological Society*, *137*(656), 553–597. https://doi.org/10.1002/qj.828

Doherty, R. M., Heal, M. R., & O'Connor, F. M. (2017). Climate change impacts on human health over Europe through its effect on air quality. *Environmental Health*, *16*(1), 33–44. https://doi.org/10.1186/s12940-017-0325-2

Fonseca, M. G., Alves, L. M., Aguiar, A. P. D., Arai, E., Anderson, L. O., Rosan, T. M., et al. (2019). Effects of climate and land-use change scenarios on fire probability during the 21st century in the Brazilian Amazon. *Global Change Biology*, *25*(9), 2931–2946. https://doi.org/10.1111/gcb.14709

Global Forest Watch (2019). Brazil Biomes. http://data.globalforestwatch.org/datasets/54ec099791644be4b273d9d8a853d452_4/data

Hansen, M. C., Potapov, P. V., Moore, R., Hancher, M., Turubanova, S. A., Tyukavina, A., et al. (2013). High-resolution global maps of 21st-century forest cover change. *Science*, *342*(6160), 850–853. https://doi.org/10.1126/science.1244693

Hodgson, A. K., Morgan, W. T., O'Shea, S., Bauguitte, S., Allan, J. D., Darbyshire, E., et al. (2018). Near-field emission profiling of tropical forest and Cerrado fires in Brazil during SAMBBA 2012. *Atmospheric Chemistry and Physics*, *18*(8), 5619–5638. https://doi.org/10.5194/acp-18-5619-2018

Hollaway, M. J., Arnold, S. R., Challinor, A. J., & Emberson, L. D. (2012). Intercontinental trans-boundary contributions to ozone-induced crop yield losses in the North Hemisphere. *Biogeosciences*, *9*, 271–2929. https://doi.org/10.5194/bg-9-271-2012

Hosely, R. M., Smith, S. J., Feng, L., Kllmont, Z., Janssens-Maenhout, G., Pitkanen, T., et al. (2018). Historical (1750–2014) anthropogenic emissions of reactive gases and aerosols from the Community Emissions Data System (CEDS). *Geoscientific Model Development*, *11*(1), 369–408. https://doi.org/10.5194/gmd-11-369-2018

Jacobson, L. S. V., Hacon, S. S., Castro, H. A., Ignotti, E., Artaxo, P., Saldiva, P. H. N., & de Leon, A. C. M. P. (2014). Acute effects of particulate matter and black carbon from seasonal fires on peak expiratory flow of school children in the Brazilian Amazon. *Public Library of Science*, *9*(8), 1, e104177–14. https://doi.org/10.1371/journal.pone.0104177

Jaffe, D. A., & Wigder, N. L. (2012). Ozone production from wildfires: A critical review. *Atmospheric Environment*, *51*, 1–10. https://doi.org/10.1016/j.atmosenv.2011.11.063

Jerrett, M., Burnett, R. T., Pope, C. A., Ito, K., Thurston, G., Krewski, D., et al. (2009). Long-term ozone exposure and mortality. *The New England Journal of Medicine*, *360*(11), 1085–1095. https://doi.org/10.1056/NEJMoa0803894

Johnston, F. H., Henderson, S. B., Chen, Y., Randerson, J. T., Marlier, M., Defries, R. S., et al. (2012). Estimated global mortality attributable to smoke from landscape fires. *Environmental Health Perspectives*, *120*(5), 695–701. https://doi.org/10.1289/ehp.1104422

Kaiser, J. W., Hell, A., Andreae, M. O., Benedetti, A., Chubarova, N., Jones, L., et al. (2012). Biomass burning emissions estimated with a global fire assimilation system based on observed fire radiative power. *Biogeosciences*, *9*(1), 527–554. https://doi.org/10.5194/bg-9-527-2012

Kirchhoff, V. W. J. H., Alves, J. R., da Silva, F. R., & Fishman, J. (1996). Observations of ozone concentrations in the Brazilian Cerrado during the TRACE A field expedition. *Journal of Geophysical Research*, *101*(D19), 24,029–24,042. https://doi.org/10.1029/95JD03030

Kirchhoff, V. W. J. H., & Marinho, E. V. A. (1994). Layer enhancements of tropospheric ozone in regions of biomass burning. *Atmospheric Environment*, *28*(1), 69–74. https://doi.org/10.1016/1352-2310(94)90023-X

Kolusu, S. R., Marsham, J. H., Mulcahy, J., Dunning, C., Bush, M., & Spracklen, D. V. (2015). Impacts of Amazonian biomass burning aerosols assessed from short-range weather forecasts. *Atmospheric Chemistry and Physics*, *15*, 12,251–12,266. https://doi.org/10.5194/acp-15-12251-2015

Longo, K. M., Freitas, S. R., Andreae, M. O., Yokelson, R. & Artaxo, P. (2009). Biomass burning in Amazonia: Emissions, long-range transport of smoke, and its regional and remote impacts (Amazonia and Global Change, Volume 186).

Mann, G. W., Carslaw, K. S., Spracklen, D. V., Ridley, D. A., Manktelow, P. T., Chipperfield, M. P., et al. (2010). Description and evaluation of GLOMAP-mode: A modal global aerosol microphysics model for the UKCA composition-climate model. *Geoscientific Model Development*, *3*(2), 519–551. https://doi.org/10.5194/gmd-3-519-2010

Miles, G. M., Siddans, R., Kerridge, B. J., Latter, B. G., & Richards, N. A. D. (2015). Tropospheric ozone and ozone profiles retrieved from GOME-2 and their validation. *Atmospheric Measurement Techniques*, *8*, 385–398. https://doi.org/10.5194/amt-8-385-2015

Monks, S. A., Arnold, S. R., Hollaway, M. J., Pope, R. J., Wilson, C., Feng, W., et al. (2017). The TOMCAT global chemistry transport model v1.6: Description of chemical mechanism and model evaluation. *Geoscientific Model Development*, *10*(8), 3025–3057. https://doi.org/10.5194/gmd-10-3025-2017

Morgenstern, O., Hegglin, M. I., Rozanov, E., O'Connor, F. M., Abraham, N. L., Akiyoshi, H., et al. (2017). Review of the global models used with phase 1 of the Chemistry-Climate Model Initiative (CCMI). *Geoscientific Model Development*, *10*(2), 639–671. https://doi.org/10.5194/gmd-10-639-2017

Moxim, W. J., & Levy, H. (2000). A model analysis of tropical South Atlantic Ocean tropospheric ozone maximum: The interaction of transport and chemistry. *Journal of Geophysical Research*, *105*(D13), 17,393–17,415. https://doi.org/10.1029/2000JD900175

NASA (2019). Uptick in Amazon Fire Activity in 2019. https://www.earthobservatory.nasa.gov/images/145498/uptick-in-amazon-fire-activity-in-2019.

Pacifico, F., Folberth, G. A., Sitch, S., Haywood, J. M., Rizzo, L. V., Malavelle, F. F., & Artaxo, P. (2015). Biomass burning related ozone damage on vegetation over the Amazon forest: A model sensitivity study. *Atmospheric Chemistry and Physics*, *15*, 2791–2804. https://doi.org/10.5194/acp-15-2791-2015

Page, Y. L., Morton, D., Hartin, C., Bond-Lamberty, B., Pereira, J. M. C., & Hurtt, G., & Asrar, G. (2017). Synergy between land use and climate change increases future fire risk in Amazon forests. *Earth System Dynamics*, *8*, 1237–1246. https://doi.org/10.5194/esd-8-1237-2017

Pope, R. J., Arnold, S. R., Chipperfield, M. P., Latter, B. G., Siddans, R., & Kerridge, B. J. (2018). Widespread changes in UK air quality observed from space. *Atmospheric Science Letters*, *19*, e817. https://doi.org/10.1002/asl.817

Reddington, C. L., Butt, E. W., Ridley, D. A., Artaxo, P., Morgan, W. T., Coe, H., & Spracklen, D. V. (2015). Air quality and human health improvements from reductions in deforestation-related fires in Brazil. *Nature Geoscience*, *8*, 768–773. https://doi.org/10.1038/ngeo2535

Reddington, C. L., Spracklen, D. V., Artaxo, P., Ridley, D. A., Rizzo, L. V., & Arana, A. (2016). Analysis of particulate emissions from tropical biomass burning using a global aerosol model and long-term surface observations. *Atmospheric Chemistry and Physics*, *16*(17), 11083–11106. https://doi.org/10.5194/ACP-16-11083-2016

Remer, L. A., Kaufman, Y. J., Tanré, D., Mattoo, S., Chu, D. A., Martins, J. V., et al. (2005). The MODIS aerosol algorithm, products and validation. *Journal of the Atmospheric Sciences*, *62*(4), 947–973. https://doi.org/10.1175/JAS3385.1

Santo, M. A., Filho, J. B. S. F., Filho, J. E. R. V., & Ywata, A. X. C. (2017). Setor Agropecuário Brasileiro Pós-Novo Código Florestal: Uma simulação de impactos econômicos. *Instituto de Pesquisa Econômica Aplicada*, *2320*, 1–46.

Scott, C. E., Monks, S. A., Spracklen, D. V., Arnold, S. R., Forster, P. M., Rap, A., et al. (2018). Impacts on short-lived climate forcers increases projected warming due to deforestation. *Nature Communications*, *9*(1), 157. https://doi.org/10.1038/s41467-017-02412-4

Sena, E. T., & Artaxo, P. (2015). A novel methodology for large-scale daily assessment of direct radiative forcing of smoke aerosols. *Atmospheric Chemistry and Physics*, *15*, 5471–5483. https://doi.org/10.5194/acp-15-5471-2015

Sitch, S., Cox, P. M., Collins, W. J., & Huntingford, C. (2007). Indirect radiative forcing of climate change through ozone effects on the land carbon sink. *Nature*, *448*, 791–795. https://doi.org/10.1038/nature06059

Terrabrasilia. (2019). Analyses – Legal Amazon. http://terrabrasilis.dpi.inpe.br/app/dashboard/alerts/legal/amazon/aggregated/

Thornhill, G. D., Ryder, C. L., Highwood, E. J., Shaffrey, L. C., & Johnson, B. T. (2018). The effect of South American biomass burning aerosol emissions on regional climate. *Atmospheric Chemistry and Physics*, *18*, 5321–5342. https://doi.org/10.5194/acp-18-5321-2018

United Nations (UN) (2017). World population prospects: The 2017 revisions-key finds and advice tables.

van der Werf, G. R., Randerson, J. T., Giglio, L., van Leeuwen, T. T., Chen, Y., Rogers, B. M., et al. (2017). Global fire emission estimates during 1997–2016. *Earth System Science Data*, *9*(2), 697–720. https://doi.org/10.5194/essd-9-697-2017

Van Dingenen, R., Dentener, F. J., Raes, F., Krol, M. C., Emberson, L., & Cofala, J. (2009). The global impact of ozone on agriculture crop yields under current and future air quality legislation. *Atmospheric Environment*, *43*(3), 604–618. https://doi.org/10.1016/j.atmosenv.2008.10.033

Ward, D. E., Susott, R. A., Kauffman, J. B., Babbitt, R. E., Cummings, D. L., Dias, B., et al. (1992). Smoke and fire characteristics for Cerrado and deforestation burns in Brazil: BASE-B Experiment. *Journal of Geophysical Research*, *97*(D13), 14,601–14,619. https://doi.org/10.1029/92JD01218

Wooster, M. J., Gaveau, D. L. A., Salim, M. A., Zhang, T., Xu, W., Green, D. C., et al. (2018). New tropical peatland gas and particulate emissions factors indicate 2015 Indonesian fires release far more particulate matter (but less methane) than current inventories imply. *Remote Sensing*, *10*(4), 495. https://doi.org/10.3390/rs10040495